

Article

Protection of Carbon Steel Rebars by Epoxy Coating with Smart Environmentally Friendly Microcapsules

Jacob Ress , Ulises Martin , Juan Bosch  and David M. Bastidas * 

National Center for Education and Research on Corrosion and Materials Performance, NCERCAMP-UA, Dept. Chemical, Biomolecular, and Corrosion Engineering, The University of Akron, 302 E Buchtel Ave, Akron, OH 44325-3906, USA; jtr45@zips.uakron.edu (J.R.); um11@zips.uakron.edu (U.M.); jb394@zips.uakron.edu (J.B.)

* Correspondence: dbastidas@uakron.edu; Tel.: +1-330-972-2968

Abstract: The protection of mild steel by modified epoxy coating containing colophony microencapsulated corrosion inhibitors was investigated in this study. The corrosion behavior of these epoxy coatings containing colophony microcapsules was studied by electrochemical analysis using cyclic potentiodynamic polarization and electrochemical impedance spectroscopy. The microcapsule coating showed decreased corrosion current densities of 2.75×10^{-8} and 3.21×10^{-8} A/cm² along with corrosion potential values of 0.349 and 0.392 V_{SCE} for simulated concrete pore solution and deionized water with 3.5 wt.% NaCl, respectively, indicating improved corrosion protection in both alkaline and neutral pH. Electrochemical impedance spectroscopy analysis also showed charge transfer resistance values over one order of magnitude higher than the control sample, corroborating the electrochemical corrosion potential and current density testing results. Overall, the use of colophony microcapsules showed improved corrosion protection in simulated concrete pore solution and DI water solutions containing chloride ions.

Keywords: smart corrosion inhibitors; epoxy coating; simulated concrete pore solution; microcapsules; chlorides; double emulsion



Citation: Ress, J.; Martin, U.; Bosch, J.; Bastidas, D.M. Protection of Carbon Steel Rebars by Epoxy Coating with Smart Environmentally Friendly Microcapsules. *Coatings* **2021**, *11*, 113. <https://doi.org/10.3390/coatings11020113>

Received: 31 December 2020

Accepted: 19 January 2021

Published: 20 January 2021

Publisher's Note: MDPI stays neutral with regard to jurisdictional claims in published maps and institutional affiliations.



Copyright: © 2021 by the authors. Licensee MDPI, Basel, Switzerland. This article is an open access article distributed under the terms and conditions of the Creative Commons Attribution (CC BY) license (<https://creativecommons.org/licenses/by/4.0/>).

1. Introduction

Reinforced concrete structures are an integral component in the construction industry due to their excellent mechanical properties and formability [1]. However, due to the porous nature of concrete, reinforced structures are prone to environmental degradation, leading to premature failure. The failure of these reinforced concrete structures is commonly caused by the corrosion of steel rebar reinforcements. Corrosion of concrete reinforcements presents the most significant source of deterioration of concrete structures, presenting major concerns for safety, cost, and structure lifetime [2,3]. The alkaline environment of the concrete protects steel reinforcements by the development of a passive oxide film. However, carbonation and the ingress of aggressive ions, such as chlorides, cause passivity breakdown and initiation of steel corrosion [4,5].

Protection from these aggressive agents and, therefore, corrosion of the reinforcements have been widely studied and various methods have been used. The protection measures employed include the use of stainless steel reinforcements [6–9], the use of corrosion inhibitors [10–12], decreasing the porosity of the concrete [13], and applying corrosion protective coatings on steel reinforcements [14,15]. Coatings present a particularly appealing corrosion mitigation method due to their ability to not only serve as a protective barrier, but also to house beneficial additives such as inhibitors, self-healing agents, among others [16–18]. The most common coating used for protection of concrete reinforcements is epoxy coating, which is widely available and has been proven successful [19]. However, the brittle nature of dried epoxy coatings negates the positive effects of the coating, allowing the initiation of corrosion on the reinforcement.

To combat the failures of epoxy coatings, self-healing epoxy coatings and coatings containing anticorrosion agents have been developed. In a recent work by Sharma et al., epoxy coatings containing nanoclay and tung oil were developed and were found to enhance the self-healing capabilities of the coating as well as improve its corrosion resistance [20]. Additionally, Yang et al. studied an epoxy coating modified with nanoparticles functionalized with corrosion inhibitors, which was found to improve corrosion protection in 3.5 wt.% NaCl on mild steel [21].

Recently, microcapsules and nanoparticles have been of particular interest in the study of corrosion protection of steel-reinforced concrete [22–24]. Dong et al. utilized cellulose-based microcapsules containing nitrites to delay depassivation of the concrete reinforcements [25]. The use of microcapsules in coatings to develop smart technologies which react with specific triggers has been a large area of interest in recent years. Specifically, Ouarga et al. developed an anticorrosion coating containing phosphorylated ethyl cellulose microcapsules, which enhanced the corrosion protection of mild steel in chloride solution [26]. However, few studies have been performed to evaluate the viability of microcapsules containing corrosion inhibitors in protective coatings for use in a concrete environment.

In this work, a novel epoxy coating containing pH-sensitive colophony microencapsulated corrosion inhibitors was developed and its corrosion behavior studied. The coating was fabricated with the addition of colophony microcapsules containing NaNO₂ corrosion inhibitors. The modified coating was imaged by scanning electron microscope (SEM) and corrosion behavior was tested in simulated concrete pore solution and deionized water contaminated with 3.5 wt.% NaCl.

2. Materials and Methods

Carbon steel specimens were used, the composition of which is shown in Table 1. Smart microcapsules containing NaNO₂ corrosion inhibitor were synthesized according to the double-emulsion process in previous work by the authors [10]. First, colophony (pine resin) was dissolved in diethyl ether (Sigma Aldrich, 99%, St. Louis, MO, USA) to create the organic phase for the outer shell. Next, aqueous solutions of NaNO₂ and polyvinyl alcohol (PVA) were added dropwise under stirring to form the first emulsion. Afterwards, a solution of 4 wt.% PVA was added dropwise under reduced stirring to form the double emulsion and the diethyl ether was evaporated by heating the solution to 50 °C under stirring. The PVA was used as a steric emulsion-stabilizing agent due to its ability to deter coalescence in double emulsions [27]. The microcapsules were washed with DI water, filtered, and added to the Valspar Greenbar epoxy coating during the addition of cross linker and resin. The coating was applied on the carbon steel panel using a draw-down bar. The coating was cured and dried in air for 24 h before testing. The coating thickness was approximately 110 ± 8 µm, measured by an Elcometer 311 Gauge thickness. Ten thickness measurements were taken for each specimen, and it was found that the microcapsules did not have a significant effect on the coating thickness. Blank samples were prepared without the addition of microcapsules.

Table 1. The composition of carbon steel specimens.

C	Mn	P	S	Si	Cu	Ni	Cr	Mo	V	Fe
0.38	1.08	0.019	0.043	0.20	0.37	0.16	0.16	0.050	0.0379	Bal.

Scanning electron microscopy (SEM) was used to obtain the general size and morphology of the microcapsules using a Hitachi TM3030+ SEM (Hitachi High-Tech America Inc, Schaumburg, IL, USA) with the back scattered electron technique, using a 15 kV excitation voltage and a working distance of 8 µm. Additionally, the coating with and without microcapsules was examined by SEM with the addition of energy dispersive X-ray (EDX) spectroscopy for elemental composition analysis. Water absorption tests were conducted

on microcapsule (MC) specimens and blank specimens without MC addition by measuring the weight change after exposure to deionized water for up to 20 days.

Electrochemical characterization was performed in 3.5 wt.% NaCl solution at pH 6.8 and 12.6 using DI water and simulated concrete pore solution (SCPS), respectively. Gamry Series 600 potentiostat and a standard three-electrode cell setup were used. The reference electrode used was a saturated calomel electrode (SCE), the counter electrode used was a graphite rod with a large area exposed, and the working electrode was the coated and uncoated carbon steel panels. Electrochemical corrosion monitoring was performed on samples coated with epoxy coating and epoxy coating with microcapsules every 2 days for 15 days. Open-circuit potential (OCP) was first obtained over a period of 1 h to achieve a steady-state potential. Subsequently, EIS was performed at OCP between the frequencies of 10^6 and 10^{-2} Hz with 10 mV r.m.s. and recording 10 points per decade. Lastly, potentiodynamic polarization (PP) was performed using a scan range from -0.5 and $+0.5$ V_{OCP}, with a scan rate of 0.1667 mV/s. All tests were performed in triplicate to ensure reproducibility.

3. Results

Figure 1 shows dried colophony microcapsules and their size distribution for use in the epoxy coating. The microcapsules show a spherical morphology with some pores present on the surface. Additionally, as the microcapsules are dried, agglomeration is seen. This behavior is not observed in suspension nor during the addition to the epoxy coating and coating application. The average size of the microcapsule was 51 μm in diameter, with the majority of microcapsules below 100 μm in diameter. Figure 2a shows the elemental mapping by EDX spectroscopy of the image in Figure 2m, showing an abundance of carbon, oxygen, silicon, and titanium from the epoxy coating. Additionally, areas enriched in calcium, magnesium, phosphorous and sodium can be observed along with trace amounts of nitrogen, chlorine, iron, and potassium. The spectrum in Figure 2n shows a significant amount of carbon compared to the other elements due to carbon being the major component of the epoxy coating. With the addition of colophony microcapsules, Figure 3a–l shows the EDX analysis, corresponding to the loaded coating incorporating the smart microencapsulated NaNO_2 corrosion inhibitors shown in Figure 3m, and the EDX spectrum is presented in Figure 3n. A large microcapsule can be observed in the middle of Figure 3m, in which an area enriched in sodium, potassium, oxygen, and chloride is shown. This change in atomic concentration of these species is caused by the interactions of the ionic species with the abietic acid during the mixing and curing process of the coating application [28,29].

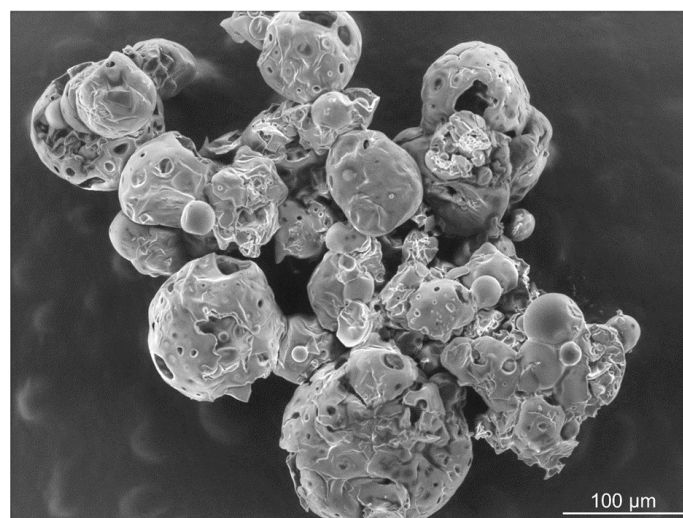


Figure 1. SEM micrograph of colophony microcapsules added to modify the epoxy coating.

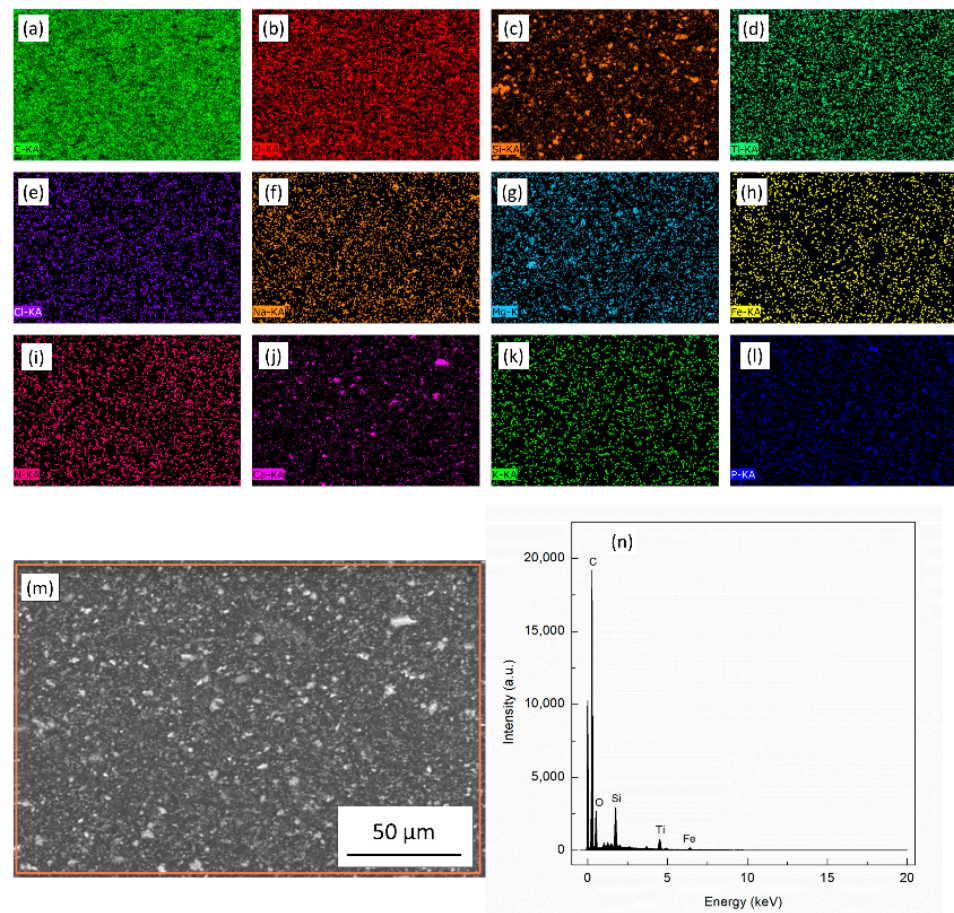


Figure 2. EDX mapping for (a) carbon, (b) oxygen, (c) silicon, (d) titanium, (e) chlorine, (f) sodium, (g) magnesium, (h) iron, (i) nitrogen, (j) calcium, (k) potassium, and (l) phosphorus for the epoxy coating on carbon steel plates. The SEM micrograph (m) displays the area analyzed and the spectrum with major peaks is shown in (n).

The surface analysis by infinite focus microscopy (IFM) can be seen in Figure 4a,b for the coating with and without addition of microcapsules, respectively. In the coating, some larger microcapsules can be observed by a 6 μm bump in the surface, compared to the normal height variations of nearly $\pm 1 \mu\text{m}$ with no microcapsules. This small increase in coating height will be particularly imperceptible after the addition of a topcoat above the epoxy primer.

The water uptake study of the coating can be seen in Figure 5. After 550 h of exposure, the coating showed a total weight gain of 10 mg, higher than the coating containing no microcapsules. This increased water adsorption is due to the increased porosity of the coating due to the voids created by the microcapsules after release of the inhibitor solution contained in the microcapsules. The increased water absorption may have a detrimental effect on the adhesion properties of the coating. However, the resistance values measured in the electrochemical monitoring in Figure 6 show improved corrosion resistance over the time period measured. Overall, the microcapsule coating displayed resistance values nearly one order of magnitude higher than the coating without microcapsules.

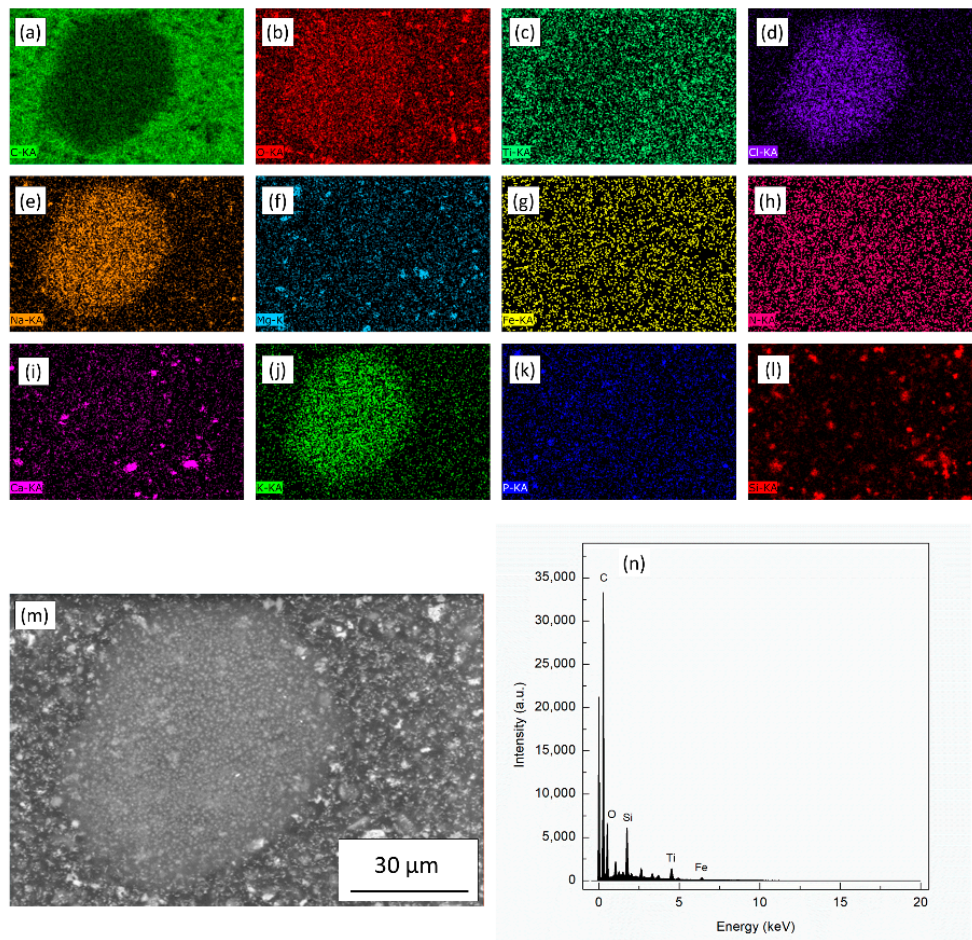


Figure 3. EDX mapping for (a) carbon, (b) oxygen, (c) titanium, (d) chlorine, (e) sodium, (f) magnesium, (g) iron, (h) nitrogen, (i) calcium, (j) potassium, (k) phosphorus, and (l) silicon for the epoxy coating on carbon steel plates containing colophony microcapsules. The SEM micrograph (m) displays the area analyzed and the spectrum with major peaks is shown in (n).

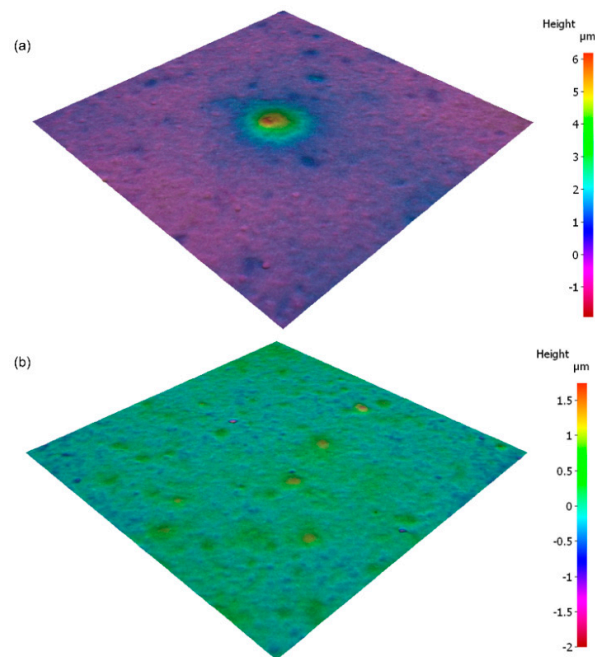


Figure 4. Infinite focus micrographs for (a) epoxy coating containing microcapsules, and (b) epoxy coating with no microcapsules.

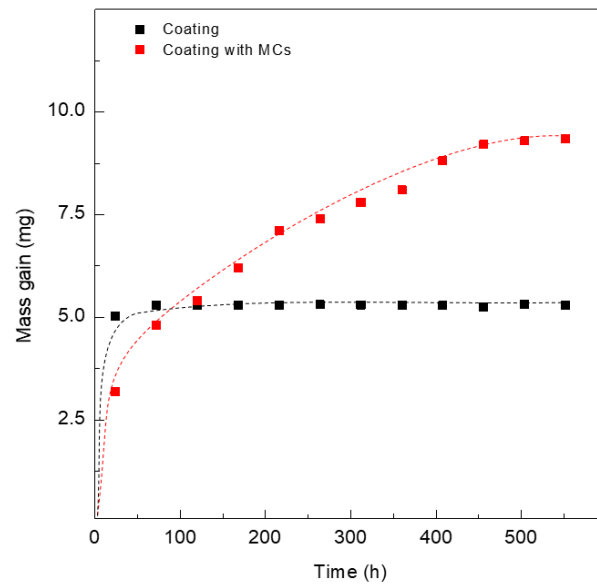


Figure 5. The water uptake of Valspar Greenbar coating with microcapsules (MCs) and without microcapsules (blank) on carbon steel plates measured by mass change.

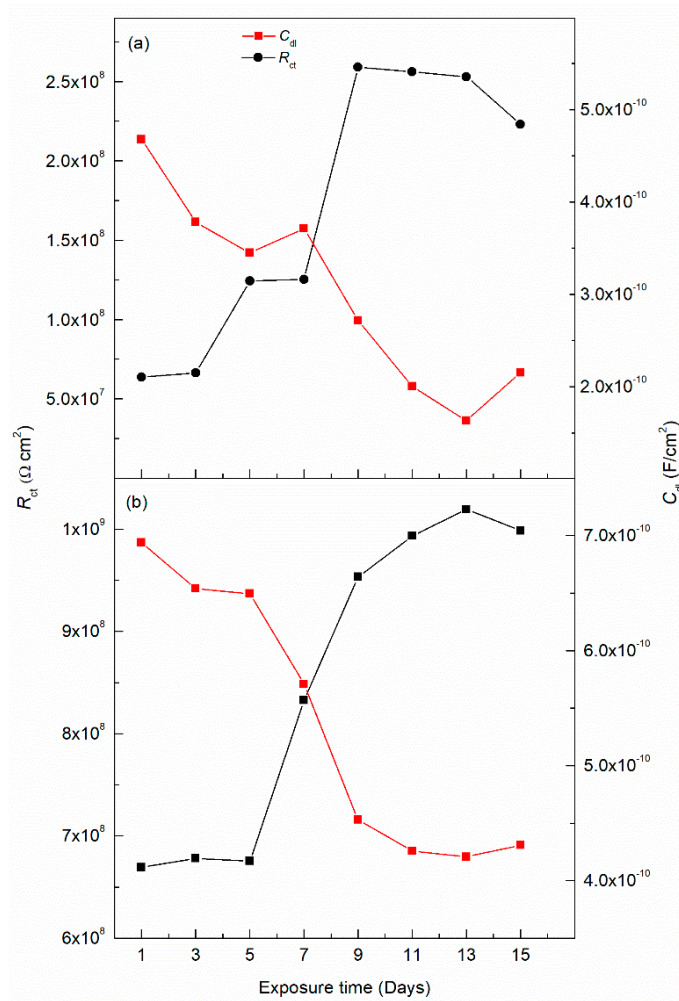


Figure 6. The resistance and capacitance monitoring of specimens (a) without microcapsules, and (b) with microcapsules in 3.5 wt.% NaCl measured by EIS.

Figure 7 shows the PP curves for the modified epoxy coating in DI water and SCPS contaminated with 3.5 wt.% NaCl. Table 2 shows the electrochemical parameters, corrosion potential (E_{corr}), corrosion current density (i_{corr}), anodic Tafel slope (β_a), and cathodic Tafel slope (β_c) values obtained from the PP curves via Tafel analysis. In 3.5 wt.% NaCl DI water solution, a more noble E_{corr} value was recorded, $-0.392 \text{ V}_{\text{SCE}}$, compared to the control steel sample, $-0.683 \text{ V}_{\text{SCE}}$. Additionally, the i_{corr} values for the coated sample display significantly lower value, approximately two orders of magnitude lower than the control sample, thus showing the increased protection of the modified epoxy coating. The kinetics of the corrosion reactions can be compared using the β_a and β_c values. For the specimens tested in 3.5 wt.% NaCl SCPS, the microcapsule sample exhibits a slightly increased β_a value, showing 0.736 V/dec compared to the control sample with 0.710 V/dec , thus indicating the enhanced protection of the microcapsule-containing coating from the anodic dissolution reaction. Furthermore, this increase in β_a is seen in the near neutral pH of the DI water, showing an increased β_a of 0.753 V/dec . However, the value is comparable to the obtained value in SCPS. This large change in β_a is due to the NaNO_2 corrosion inhibitors, which are anodic inhibitors and facilitate the formation of protective ferric oxide layers. This is not observed in SCPS because the protective oxide and oxyhydroxide passive film is formed spontaneously in alkaline solutions [10,30]. The enhanced protection shown in the E_{corr} and i_{corr} values offered by the microcapsule coating under aggressive conditions indicates the potential of the microcapsule coatings to increase the durability and lifetime of reinforced concrete.

Additionally, EIS analysis in SCPS and DI water containing chlorides showed increased corrosion resistance for the coating samples containing colophony microcapsules. Figure 8a displays the Nyquist plot in SCPS, the microcapsule-containing sample shows higher impedance values nearing $4 \text{ M}\Omega \text{ cm}^2$, while the control sample impedance value is only $1 \text{ k}\Omega \text{ cm}^2$. Similarly, Figure 8b shows the Nyquist plots obtained in DI water containing chlorides, also showing the microcapsule-containing samples with higher impedance values than the control. The DI water-exposed samples also display lower impedance values due to the decreased pH, thus preventing the formation of protective oxide film on any exposed steel, initiating corrosion [30]. The EIS data were fitted to the equivalent circuits shown in Figure 9a,b. The control samples, lacking microcapsules, are modeled by a two-time constant model where R_s is the solution resistance, CPE_f is the capacitance of the passive film or coating, R_f is the resistance of the passive film or coating, CPE_{dl} is the double layer capacitance, and R_{ct} is the charge transfer resistance for the corrosion process. The microcapsules containing coatings, however, display an additional time constant behavior attributed to the interface between microcapsules and the coating, modeled by CPE_{MC} as the microcapsule capacitance and R_{MC} as the microcapsule resistance. Table 3 shows the fitting parameters obtained from the EIS analysis. The protective and anticorrosion effects of the microcapsule coating are highlighted by the differences in the R_f , CPE_f , R_{ct} , and CPE_{dl} , and by the appearance of a tertiary loop in the circuit to represent the microcapsules. The R_f shows a substantial increase in both SCPS and DI water solutions from 1710 and $65 \text{ }\Omega \text{ cm}^2$ for the control in SCPS and DI, respectively, to 1.93×10^5 and $5.55 \times 10^5 \text{ }\Omega \text{ cm}^2$ for the microcapsule coating specimens. The larger R_f shown by the DI water-exposed specimens is attributed to the porosity increase in the coating due to the partial dissolution of the microcapsules in alkaline environments, which releases the inhibitors [10]. Similarly, the R_{ct} values show an order of magnitude increase for the microcapsule coating compared to the control for both solutions tested. Lastly, the addition of microcapsules causes the EEC to change, adding a time constant associated with the microcapsules in the coating, showing an additional resistance, R_{MC} , of 8.68×10^5 and $3.30 \times 10^5 \text{ }\Omega \text{ cm}^2$ for the SCPS and DI water solutions, respectively.

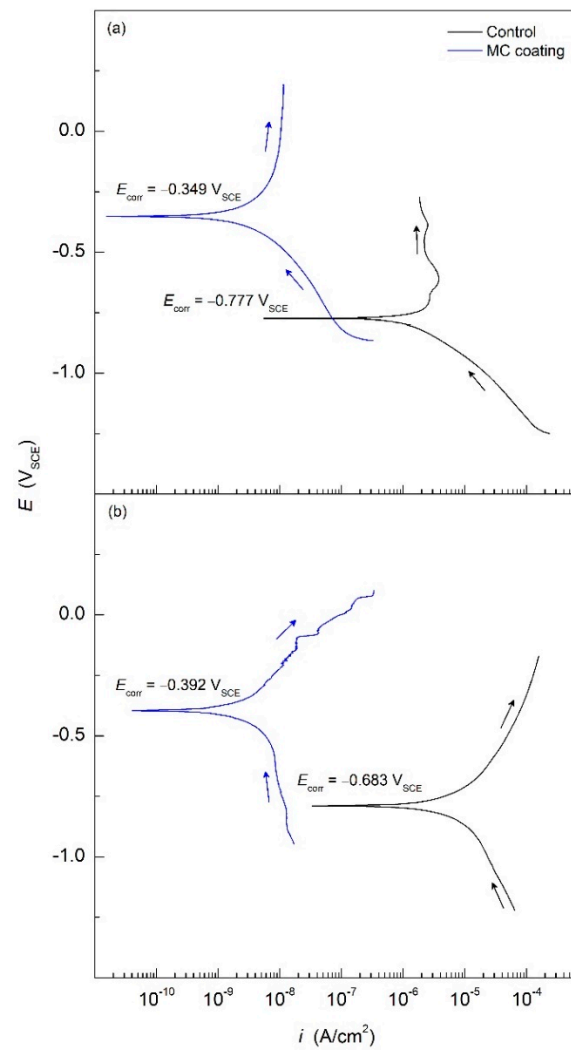


Figure 7. Potentiodynamic polarization curves for mild steel with epoxy coating modified with colophony microcapsules exposed to (a) simulated concrete pore solution, and (b) DI water contaminated with 3.5 wt.% NaCl.

Table 2. Electrochemical parameters calculated by Tafel fitting from potentiodynamic polarization for epoxy coating containing microcapsules in simulated concrete pore solution (pH 12.6) and DI water (pH 6.8) contaminated with 3.5 wt.% NaCl.

PH		E_{corr} V_{SCE}	I_{corr} A/cm^2	β_a V/dec	β_c V/dec
12.6	MC	0.349	2.75×10^{-8}	0.736	0.629
	Control	0.777	2.45×10^{-6}	0.710	0.576
6.8	MC	0.392	3.21×10^{-8}	0.753	0.803
	Control	0.683	6.53×10^{-6}	0.056	0.493

Table 3. EIS fitting values obtained for coated and uncoated steel panels in simulated concrete pore solution (pH 12.6) and DI water (pH 6.8) contaminated with 3.5 wt.% NaCl using the equivalent circuit presented in Figure 9.

PH	SAMPLE	R_s $\Omega \text{ cm}^2$	R_f $\Omega \text{ cm}^2$	CPE_f $\text{S cm}^{-2} \text{ S}^{n_f}$	n_f	R_{MC} $\Omega \text{ cm}^2$	CPE_{MC} $\text{S cm}^{-2} \text{ S}^{n_{MC}}$	n_{MC}	R_{ct} $\Omega \text{ cm}^2$	CPE_{dl} $\text{S cm}^{-2} \text{ S}^{n_{dl}}$	n_{dl}	χ^2
12.6	MC	41	1.93×10^5	1.21×10^{-8}	0.79	8.68×10^5	3.96×10^{-7}	0.71	2.94×10^9	5.30×10^{-7}	0.80	8.45×10^{-4}
	Control	34	1.17×10^4	7.98×10^{-4}	0.82	–	–	–	9.91×10^8	1.88×10^{-6}	0.85	1.76×10^{-4}
6.8	MC	35	5.55×10^5	1.23×10^{-8}	0.88	3.30×10^5	1.66×10^{-7}	0.79	2.70×10^9	6.21×10^{-8}	0.80	2.08×10^{-3}
	Control	29	6.50×10^3	1.17×10^{-4}	0.79	–	–	–	9.03×10^8	1.38×10^{-6}	0.88	2.16×10^{-4}

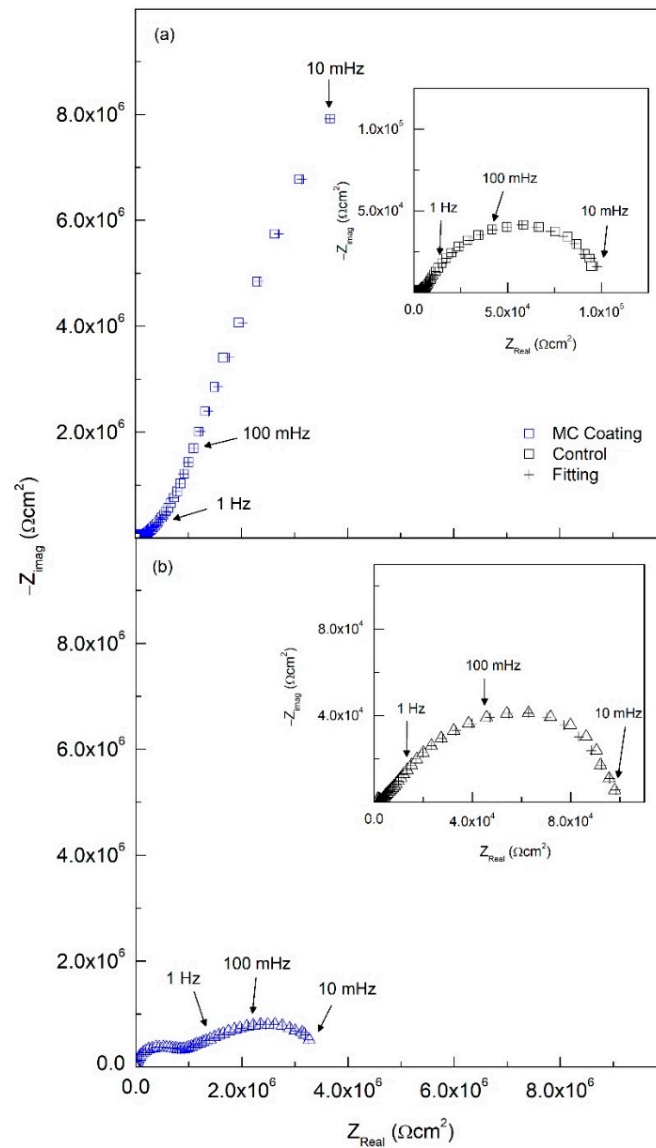


Figure 8. Nyquist plots obtained from EIS for mild steel with epoxy coating modified with colophony microcapsules exposed to (a) simulated concrete pore solution, and (b) DI water contaminated with 3.5 wt.% NaCl.

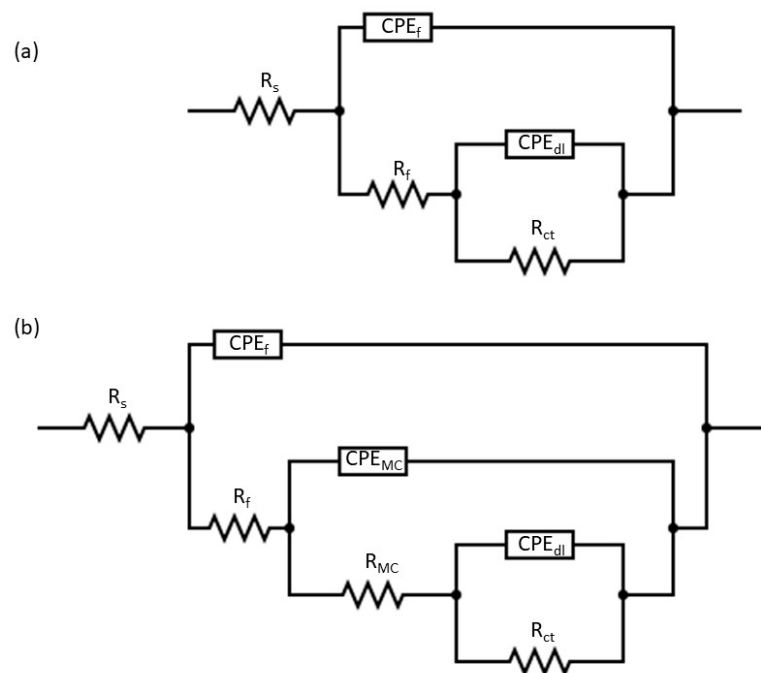


Figure 9. Electrical equivalent circuits used to fit EIS data for (a) coated specimens and (b) coated specimens with colophony microcapsules.

4. Conclusions

The use of colophony pH-sensitive microcapsules containing corrosion inhibitors in epoxy coating for protection of reinforced concrete was studied. This paper studied accelerated testing in a simulated concrete pore solution environment and the following conclusions can be drawn.

- The water absorption of the microcapsule-containing coating sample showed increased weight gain from water intake over the test period compared to epoxy coating without microcapsules. However, the resistance values obtained from EIS analysis over the same time period showed superior resistance for the microcapsule coating samples. After 15 days of exposure to DI water, R_{ct} values of the microcapsule coating displayed $1.0 \times 10^9 \Omega \text{ cm}^2$, approximately one order of magnitude higher than the coating without microcapsules.
- Additionally, PP results showed nobler E_{corr} and lower i_{corr} values for the microcapsule samples, showing improved corrosion resistance properties. In a simulated concrete environment with chloride contamination, the microcapsule coating sample measured an E_{corr} of 0.349 mV_{SCE} and an i_{corr} of $2.75 \times 10^{-8} \text{ A/cm}^2$, improving the corrosion performance of the coating.
- EIS analysis showed a three-time constant behavior for the microcapsule samples with impedance values of one order of magnitude higher than the control samples, indicating significantly improved resistance to corrosion. The microcapsule coating also measured R_{ct} values of 2.94×10^9 and $2.70 \times 10^9 \Omega \text{ cm}^2$ for pH 12.6 and pH 6.8, respectively, nearly one order of magnitude higher than the coating without microcapsules in each solution.
- Epoxy coating containing colophony microcapsules with corrosion inhibitors proves to be an effective method to improve corrosion protection of mild steel in 3.5 wt. NaCl-contaminated SCPS. Therefore, the microcapsule coating shows significant potential in enhancing the lifetime and durability of steel-reinforced concrete structures.

Author Contributions: Conceptualization, D.M.B.; methodology, J.R., U.M., J.B., and D.M.B.; formal analysis, J.R., U.M., J.B., and D.M.B.; investigation, J.R., U.M., J.B., and D.M.B.; resources, D.M.B.; data curation, J.R., U.M., J.B., and D.M.B.; writing—original draft preparation, J.R., U.M., J.B., and

D.M.B.; writing—review and editing, J.R. and D.M.B.; visualization, D.M.B.; supervision, D.M.B.; project administration, D.M.B.; funding acquisition, D.M.B. All authors have read and agreed to the published version of the manuscript.

Funding: This research was funded by Firestone Research, Grant No. 639430, and The University of Akron.

Institutional Review Board Statement: Not applicable.

Informed Consent Statement: Not applicable.

Data Availability Statement: The raw/processed data required to reproduce these findings cannot be shared at this time as the data also forms part of an ongoing study.

Acknowledgments: The authors acknowledge the technical support and facilities from The National Center for Education and Research on Corrosion and Materials Performance (NCERCMAP-UA), The College of Engineering and Polymer Science and The University of Akron.

Conflicts of Interest: The authors declare no conflict of interest.

References

1. Mehta, P.K.; Monteiro, P.J.M. *Concrete: Microstructure, Properties, and Materials*, 4th ed.; McGraw-Hill Education: New York, NY, USA, 2014.
2. Cabrera, J. Deterioration of concrete due to reinforcement steel corrosion. *Cem. Conc. Compos.* **1996**, *18*, 47–59. [[CrossRef](#)]
3. Wasim, M.; Ngo, T.; Abid, M. Investigation of long-term corrosion resistance of reinforced concrete structures constructed with various types of concretes in marine and various climate environments. *Constr. Build. Mater.* **2020**, *237*, 117701. [[CrossRef](#)]
4. Gjørsv, O.; Vennesland, Ø. Diffusion of chloride ions from seawater into concrete. *Cem. Concr. Res.* **1979**, *9*, 229–238. [[CrossRef](#)]
5. Angst, U.; Elsener, B.; Larsen, C.K.; Vennesland, Ø. Critical chloride content in reinforced concrete—A review. *Cem. Concr. Res.* **2009**, *39*, 1122–1138. [[CrossRef](#)]
6. Martin, U.; Röss, J.; Bosch, J.; Bastidas, D. Stress corrosion cracking mechanism of AISI 316LN stainless steel rebars in chloride contaminated concrete pore solution using the slow strain rate technique. *Electrochim. Acta* **2020**, *335*, 135565. [[CrossRef](#)]
7. Briz, E.; Biezma, M.V.; Bastidas, D. Stress corrosion cracking of new 2001 lean-duplex stainless steel reinforcements in chloride contained concrete pore solution: An electrochemical study. *Constr. Build. Mater.* **2018**, *192*, 1–8. [[CrossRef](#)]
8. Fajardo, S.; Bastidas, D.; Ryan, M.P.; Criado, M.; McPhail, D.; Bastidas, D.M. Low-nickel stainless steel passive film in simulated concrete pore solution: A SIMS study. *Appl. Surf. Sci.* **2010**, *256*, 6139–6143. [[CrossRef](#)]
9. Rabi, M.; Cashell, K.; Shamass, R.; Desnerck, P. Bond behaviour of austenitic stainless steel reinforced concrete. *Eng. Struct.* **2020**, *221*, 111027. [[CrossRef](#)]
10. Röss, J.; Martin, U.; Bosch, J.; Bastidas, D. pH-triggered release of NaNO₂ corrosion inhibitors from novel colophony microcapsules in simulated concrete pore solution. *ACS Appl. Mater. Interfaces* **2020**, *12*, 46686–46700. [[CrossRef](#)]
11. Bastidas, D.M.; Criado, M.; La Iglesia, V.M.; Fajardo, S.; La Iglesia, A. Comparative study of three sodium phosphates as corrosion inhibitors for steel reinforcements. *Cem. Conc. Compos.* **2013**, *43*, 31–38. [[CrossRef](#)]
12. Zhang, Z.; Ba, H.; Wu, Z. Sustainable corrosion inhibitor for steel in simulated concrete pore solution by maize gluten meal extract: Electrochemical and adsorption behavior studies. *Constr. Build. Mater.* **2019**, *227*, 117080. [[CrossRef](#)]
13. Wang, X.; Xing, F.; Zhang, M.; Han, N.; Qian, Z. Experimental study on cementitious composites embedded with organic microcapsules. *Materials* **2013**, *6*, 4064–4081. [[CrossRef](#)] [[PubMed](#)]
14. Kim, C.; Karayan, A.I.; Milla, J.; Hassan, M.M.; Castaneda, H. Smart coating embedded with pH-responsive nanocapsules containing a corrosion inhibiting agent. *ACS Appl. Mater. Interfaces* **2020**, *12*, 6451–6459. [[CrossRef](#)]
15. Du, Y.; Gao, P.; Yang, J.; Shi, F. Research on the chloride ion penetration resistance of magnesium phosphate cement (MPC) material as coating for reinforced concrete structures. *Coatings* **2020**, *10*, 1145. [[CrossRef](#)]
16. Samadzadeh, M.; Boura, S.H.; Peikari, M.; Kasirha, S.; Ashrafi, A. A review on self-healing coatings based on micro/nanocapsules. *Prog. Org. Coat.* **2010**, *68*, 159–164. [[CrossRef](#)]
17. Weishaar, A.; Carpenter, M.; Loucks, R.; Sakulich, A.; Peterson, A. Evaluation of self-healing epoxy coatings for steel reinforcement. *Constr. Build. Mater.* **2018**, *191*, 125–135. [[CrossRef](#)]
18. Afshar, A.; Jahandari, S.; Rasekh, H.; Shariati, M.; Afshar, A.; Shokrgozar, A. Corrosion resistance evaluation of rebars with various primers and coatings in concrete modified with different additives. *Constr. Build. Mater.* **2020**, *262*, 120034. [[CrossRef](#)]
19. Kepler, J.L.; Darwin, D.; Locke, C.E., Jr. Evaluation of corrosion protection methods for reinforced concrete highway structures. In *Structural Engineering and Engineering Materials*; SM Report No. 58; University of Kansas Center for Research: Lawrence, KS, USA, 2000.
20. Sharma, N.; Sharma, S.; Sharma, S.; Mehta, R. Evaluation of corrosion inhibition and self healing capabilities of nanoclay and tung oil microencapsulated epoxy coatings on rebars in concrete. *Constr. Build. Mater.* **2020**, *259*, 120278. [[CrossRef](#)]
21. Yang, W.; Feng, W.; Liao, Z.; Yang, Y.; Miao, G.; Yu, B.; Pei, X. Protection of mild steel with molecular engineered epoxy nanocomposite coatings containing corrosion inhibitor functionalized nanoparticles. *Surf. Coat. Technol.* **2020**, 126639. [[CrossRef](#)]

22. Li, K.; Liu, Z.; Wang, C.; Fan, W.; Liu, F.; Li, H.; Zhu, Y.; Wang, H. Preparation of smart coatings with self-healing and anti-wear properties by embedding PU-fly ash absorbing linseed oil microcapsules. *Prog. Org. Coat.* **2020**, *145*, 105668. [[CrossRef](#)]
23. Zuo, J.; Zhan, J.; Dong, B.; Luo, C.; Liu, Q.; Chen, D. Preparation of metal hydroxide microcapsules and the effect on pH value of concrete. *Constr. Build. Mater.* **2017**, *155*, 323–331. [[CrossRef](#)]
24. Wang, X.; Huang, Y.; Huang, Y.; Zhang, J.; Fang, C.; Yu, K.; Chen, Q.; Li, T.; Han, R.; Yang, Z.; et al. Laboratory and field study on the performance of microcapsule-based self-healing concrete in tunnel engineering. *Constr. Build. Mater.* **2019**, *220*, 90–101. [[CrossRef](#)]
25. Dong, B.; Ding, W.; Qin, S.; Han, N.; Fang, G.; Liu, Y.; Xing, F.; Hong, S. Chemical self-healing system with novel microcapsules for corrosion inhibition of rebar in concrete. *Cem. Conc. Compos.* **2018**, *85*, 83–91. [[CrossRef](#)]
26. Ouarga, A.; Noukrati, H.; Iraola-Arregui, I.; Elaissari, A.; Barroug, A.; Ben Youcef, H. Development of anti-corrosion coating based on phosphorylated ethyl cellulose microcapsules. *Prog. Org. Coat.* **2020**, *148*, 105885. [[CrossRef](#)]
27. Yang, Y.Y. Morphology, drug distribution, and in vitro release profiles of biodegradable polymeric microspheres containing protein fabricated by double-emulsion solvent extraction/evaporation method. *Biomaterials* **2001**, *22*, 231–241. [[CrossRef](#)]
28. Ren, F.; Zheng, Y.-F.; Liu, X.; Yue, X.-Y.; Ma, L.; Li, W.-G.; Lai, F.; Liu, J.-L.; Guan, W.-L. An investigation of the oxidation mechanism of abietic acid using two-dimensional infrared correlation spectroscopy. *J. Mol. Struct.* **2015**, *1084*, 236–243. [[CrossRef](#)]
29. Mantzaridis, C.; Brocas, A.-L.; Llevot, A.; Cendejas, G.; Auvergne, R.; Caillol, S.; Carlotti, S.; Cramail, H. Rosin acid oligomers as precursors of DGEBA-free epoxy resins. *Green Chem.* **2013**, *15*, 3091–3098. [[CrossRef](#)]
30. Garcés, P.; Saura, P.; Zornoza, E.; Andrade, C. Andrade, Influence of pH on the nitrite corrosion inhibition of reinforcing steel in simulated concrete pore solution. *Corros. Sci.* **2011**, *53*, 3991–4000. [[CrossRef](#)]